



Original Article

# Effects of the Application of Decellularized Amniotic Membrane Solubilized with Hyaluronic Acid on Wound Healing

MARIA EDUARDA ANASTÁCIO BORGES CORRÊA,<sup>1</sup> CAROLINI MENDES,<sup>1</sup>  
JOÃO VITOR SILVANO BITTENCOURT,<sup>1</sup> ALINE TAKEJIMA,<sup>2</sup> ISIO CARVALHO DE SOUZA,<sup>2</sup>  
SIMONE CRISTINA DIZARÓ DE CARVALHO,<sup>3</sup> INGRID GABRIELA ORLANDINI,<sup>3</sup>  
THIAGO ANTONIO MORETTI DE ANDRADE,<sup>3</sup> LUIZ CÉSAR GUARITA-SOUZA,<sup>2</sup>  
and PAULO CESAR LOCK SILVEIRA<sup>1,4</sup>

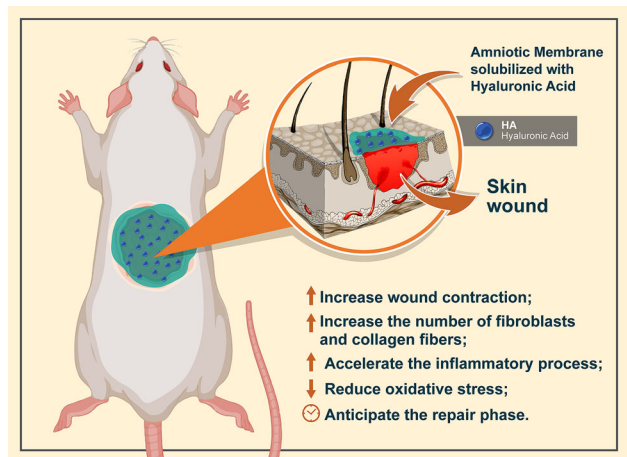
<sup>1</sup>Laboratory of Experimental Physiopathology, Program of Postgraduate in Science of Health, Universidade do Extremo Sul Catarinense, Criciúma, Santa Catarina state 88806-000, Brazil; <sup>2</sup>Experimental Laboratory of Institute of Biological and Health Sciences of Pontifical Catholic University of Paraná (PUCPR), Street Imaculada Conceição, 1155, Curitiba, Paraná 80215-901, Brazil; <sup>3</sup>Graduate Program of Biomedical Science, Herminio Ometto Foundation, Araras, SP, Brazil; and <sup>4</sup>Universidade do Extremo Sul Catarinense, Av. Universitária, 1105 Universitário – Block S, Room 16, Criciúma, SC CEP: 88806-000, Brazil

(Received 15 April 2022; accepted 3 July 2022; published online 8 July 2022)

Associate Editor Stefan M. Duma oversaw the review of this article.

**Abstract**—A perfect graft for wound care must be readily available without affecting the immune response, covering and protecting the wound bed. Considering previous studies have already established the use of hyaluronic acid (HA) for the treatment of wounds but the data presented on the amniotic membrane (AM) and its promising effects on healing still requires further investigation, this study aimed to evaluate the effects of the application of a decellularized amniotic membrane solubilized with hyaluronic acid on the healing process of cutaneous wounds on the 7th and 14th day, to evaluate the evolution of the wound and the inflammatory phases in these two times. Cutaneous lesions were excised from the dorsal region and 96 Wistar rats were divided into four groups: I—Excisional wound (EW); II—EW + AM; III—EW + HA; IV—EW + AM + HA. The present study demonstrated that the proposed combined therapy favors the tissue repair process of the epithelial lesion. Results showed a reduction in pro-inflammatory cytokines, an increase in anti-inflammatory cytokines, an increase in TGF- $\beta$ , and attenuation of oxidative stress, reducing the acute inflammatory response and promoting the beginning of tissue repair. We concluded that the proposed therapies accelerated the inflammatory process with anticipation of the repair phase.

## Graphical Abstract



**Keywords**—Amniotic membrane, Hyaluronic acid, Collagen, Fibroblasts, Oxidative stress, Wound healing.

## INTRODUCTION

It is expected that 1% of the population will experience ulcerations over their lives. Wounds impact an average of five million people in the United States

Address correspondence to Paulo Cesar Lock Silveira, Universidade do Extremo Sul Catarinense, Av. Universitária, 1105 Universitário – Block S, Room 16, Criciúma, SC CEP: 88806-000, Brazil. Electronic mail: psilveira@unesc.net

alone, and the cost of treating these wounds is estimated to be up to \$10 billion each year. An increase in the number of patients who have received insufficient treatment for chronic wounds over lengthy periods is of special concern.<sup>28</sup> Whatever the cause, wounds have a substantial but often unrecognized impact on people who suffer from them, caregivers, and the healthcare system. The phenomenon of wounds has been called the 'silent epidemic',<sup>37</sup> as it inflicts pain and suffering, lowers the life quality, raises healthcare expenses, lengthens hospital stays, and increases morbidity.<sup>19</sup>

Wounds are characterized by loss of skin integrity.<sup>32</sup> Deep wounds that destroy the epidermis and a portion of the dermis have functional consequences, such as reduced skin oxygenation and impaired tissue healing.<sup>30</sup>

Wound healing is a dynamic process that consists of four continuous, overlapping, and precisely timed phases. The events of each phase must occur in a precise and regulated manner, as any interruption or even prolongation of the process can lead to a delay in healing or a chronic wound that does not heal. Optimal wound healing involves the following events: (1) rapid hemostasis; (2) appropriate inflammation; (3) differentiation, proliferation, and migration of cells to the wound site; (4) adequate angiogenesis; (5) immediate reepithelialization and (6) adequate collagen synthesis to provide strength to the scar tissue.<sup>22</sup>

Growth factors and cytokines, such as interleukin 1 (IL-1) and tumor necrosis factor- $\alpha$  (TNF- $\alpha$ ), promote and govern the healing process. Neutrophils remove necrotic tissue and pathogens through phagocytosis and release of reactive oxygen species (ROS) in response to pro-inflammatory signals and activation of inflammatory signaling pathways (e.g., NF- $\kappa$ B).<sup>41</sup>

A perfect graft for wound care must be readily available without affecting the immune response, covering and protecting the wound bed, improving the healing process, decreasing patient pain, and resulting in little or no scar formation.<sup>18,42</sup>

The presence of several important growth factors, as well as clinically important characteristics such as anti-inflammatory behavior, angiogenic properties, epithelialization induction, antimicrobial action, and non-immunogenicity,<sup>15</sup> make the amniotic membrane (AM) a potential candidate for wound healing,<sup>16,38</sup> because its structure makes it an ideal biological material for dressings. Most of these characteristics are based on the presence of collagen types I, II, III, IV, laminin, and fibronectin in the basement membrane, in addition to growth factors (EGF, TGF $\alpha$ , and  $\beta$ , KGF, HGF, FGF, VEGF, PDGF).<sup>36</sup>

Late reepithelialization and persistent inflammation, often triggered by infections, are the primary initiators

of scar tissue development. AM also helps reduce scarring in skin wounds by secreting EGF, KGF, and HGF, which are important growth factors in epithelialization and wound healing. AM's anti-inflammatory effect is mediated through the migration inhibitory factor (MIF) and suppression of the production of pro-inflammatory cytokines such as IL1.<sup>17</sup>

Hyaluronic acid (HA), a natural polymer of the glycosaminoglycan (GAGs) family, is an attractive and profitable alternative for the creation of medical devices for the treatment of epidermal and dermal wounds.<sup>30</sup> High tissue concentrations of HA are present during the activation of essential biological processes such as remodeling, regeneration, morphogenesis and are also responsible for migration, cell differentiation, and progenitor cell tissue collection.<sup>20</sup>

Considering previous studies have already established the use of hyaluronic acid for the treatment of wounds and skin disorders, and the data presented on the amniotic membrane and its promising effects on healing that still requires further investigation, the objective of this work was to evaluate the effect of the application of decellularized amniotic membrane solubilized with hyaluronic acid in the healing process of cutaneous wounds in an experimental model of rats.

## MATERIALS AND METHODS

### *Animals*

Ninety-six male Wistar rats (2 months weighing between 250 and 300 g) were divided into two groups of 48 animals each, so that one of these groups was euthanized on the 7th and the other on the 14th day, to evaluate the entire tissue repair process, from the inflammatory to the remodeling phase. In addition, each group of 48 animals was subdivided into four groups with 12 animals each, grouped in specific cages, with a controlled room temperature between  $20 \pm /^{\circ}\text{C}$ , 12/12 h light-dark cycle, and free access, fed a standard diet for rodents and water *ad libitum*.

The animals were randomly divided into four groups with  $n = 12$  each:

- I. Excisional wound (EW);
- II. EW + hyaluronic acid (HA) 0.9%;
- III. EW + amniotic membrane (AM);
- IV. EW + AM + HA.

### *Excisional Wound Model*

The excisional wound model was induced as described by Mendes *et al.*<sup>32</sup> Animals were anesthetized

with 4% isoflurane. The dorsal region of each animal was trichotomized, cleaned, and disinfected with 70% alcohol. The medial-dorsal region, between the interscapular line and the tail, was removed with a circular surgical incision with a diameter of approximately 2 cm. The wounds were uniform in diameter, depth, and location.

#### *Amniotic Membrane*

Amniotic membranes were obtained from parturients ( $n = 2$ , with 36–40 weeks of gestational age) following approval by the ethics committee (CEUA-PUCPR) under protocol 01288. After collection, the membranes were processed within 6–12 h after normal delivery.

Decellularization of the amniotic matrix was performed using an aseptic technique, according to the methodology described by Hopper *et al.*<sup>23</sup> The effectiveness of the decellularization process was confirmed by sampling in histological analysis with HE staining and scanning electron microscopy (MEV) according to Jorge *et al.*<sup>25</sup>

#### *Treatment*

First, solubilization of AM with HA (0.9%) was performed by immersion of the membrane in hyaluronic acid (1 mL) for an hour. No tests were performed on the stability of AM with HA for reasons that a single solution was not made with the two components, but a topical application of AM solubilized by immersion of the membrane in hyaluronic acid.

In animals of group II, HA (0.9%) was applied topically to the wound. HA used was high-molecular-weight HA, above 1000 kDa, based on the work of Corrêa *et al.*<sup>11</sup> and Mendes *et al.*<sup>32</sup>

As for groups III and IV, the wound bed was completely covered by AM and/or HA (0.9%). The size/amount of membrane used was related to the size of the wound, which was a diameter of 2 cm.

After the application of treatments, all animals had the induced wounds covered with a transparent and adhesive dressing (Tegaderm). These applications were made only once.

The effectiveness of the protocol was evaluated after a healing period of 7 days in half of the animals and 14 days in the other half, aiming to evaluate the evolution of the wound and the inflammatory phases in these two times.

After these procedures, the animals were anesthetized with 4% isoflurane and killed by guillotine decapitation on the 7th and 14th days of treatment.

#### *Sample Preparation for Biochemical and Molecular Analysis*

The outer edge of the wound of eight animals per group was surgically removed, processed, and stored in a freezer at  $-80^{\circ}\text{C}$  for subsequent biochemical and molecular analysis.

#### *Wound Size Analysis*

The photographic method is a precise alternative to measure the wound area, being an appropriate technique for clean wounds, contaminated or not. Digital images of the wounds were taken at the resolution of  $3264 \times 2448$  pixels and analyzed by the ImageJ® 1.51 software. The images of the lesions were obtained on days 0, 7, and 14, and the number of animals photographed per group was  $N = 12$ , for visual verification of the evolution of the healing process and measurement of the size (length and width) calculating the variation of the areas of wounds in this period in  $\text{cm}^2$ . These measurements were made by the same researcher, three measurements were made for each wound, and the average value was used.

#### *Histological Analyses*

The wound samples of four animals per group were conditioned for 48 h in a 10% formaldehyde buffered solution (pH 7.4 phosphate buffer), followed by histological processing, and were then embedded in paraffin. Thereafter,  $5.0 \mu\text{m}$  sections were subjected simultaneously to respective hematoxylin and eosin (HE) staining, to quantify the inflammatory infiltrate, blood vessels, and fibroblasts. Moreover, Ponceau S staining was performed to quantify the percentage area of total collagen compaction.<sup>3,24,40</sup>

Furthermore, all histological sections were visualized in the LEICA® DM-2000B optical microscope with a LEICA® DFC-300 FX camera connected to the computer with LAS® software—Leica Application Suite (version 3.3.0), to capture the images.

For simultaneous quantification (evaluated by a trained pathologist) of the inflammatory infiltrate and fibroblasts, the “Cell Counter” plug-in of the ImageJ software (five images/animal/time/treatment in  $\times 400$  magnification) was used, and for blood vessels quantification at  $\times 200$  magnification (HE stain). To quantify the percentage area of total collagen compaction (stained area in red: total collagen compaction stained by Ponceau S) at  $\times 400$  (five images/animal/time/treatment), the “Color deconvolution” plug-in from ImageJ software was used (“Vector” <FastRed FastBlue DAB>).<sup>12</sup>

### RT-qPCR

Gene expression analyses of NF- $\kappa$ B and Nrf2 markers were performed using PCR—Real-Time, in samples from the 7th day after treatment.  $\beta$ -Actin was used as reference gene for normalization. Relative expression levels were determined with 7500 Fast Real-Time System Sequence Detection Software v.2.0.5 (Applied Biosystems). Relative mRNA expression levels were determined using the target/actin method. Total RNA was extracted using TRIzol® reagent (Life Technologies) and following the manufacturer's recommended instructions. The RNA obtained was solubilized in 30  $\mu$ l of Milli-Q water treated with 0.1% DEPC (Sigma), grouped in a single tube, and stored at  $-20^{\circ}\text{C}$ . Total extracted RNA was quantified by spectrophotometry in absorbance at 260 nm and 280 nm. The 260/280 nm absorbance ratio was used to estimate protein contamination. RNAs whose 260/280 nm ratio were between 1.8 and 2.0 were considered to be of good quality. Soon after, complementary DNA was synthesized using M-MLV reverse transcriptase, which promotes a complementary DNA strand from single-stranded RNA. The final part included real-time polymerase chain reaction (PCR) using the SYBR Green dye system, which has highly specific binding to double-stranded DNA, to detect the PCR product as it accumulates during cycles of the reaction.

### Determination of the Cytokine Content Using ELISA

The samples were processed and then the plate was sensitized for further incubation with the antibody. To measure cytokines (TNF- $\alpha$ , IL-1 $\beta$ , IL-6, IL-4, IL-10, TGF- $\beta$ ) the enzyme-linked immunoabsorbent assay (Duoset ELISA) capture method (R&D system, Inc., Minneapolis, USA) was used.

### Intracellular Determination of Reactive Oxygen Species (ROS) and Nitric Oxide

The intracellular levels of oxidized 2,7-dichlorofluorescein (DCF) were monitored at excitation and emission wavelengths of 488 and 525 nm, as described by Dong.<sup>13</sup> The endothelial function was assessed by evaluating the nitric oxide levels by measuring its stable nitrite metabolite, and quantified by spectrophotometer at 540 nm as described in the literature.<sup>9</sup>

### Determination of Oxidative Damage Marker Levels

The oxidative damage to protein was measured by the determination of carbonyl groups, based on a reaction with dinitrophenylhydrazine (DNTP), and the

carbonyl contents were determined by measuring the absorbance at 370 nm.<sup>27</sup>

Total thiol content was determined using the 5,5-dithiobis (2-nitrobenzoic acid) (2-nitrobenzoic acid) (DTNB) method, the absorbance at 412 nm was measured, and the amount of TNB formed (equivalent to the amount of sulfhydryl (SH) groups) was calculated.<sup>1</sup>

### Determination of Antioxidant Defenses

Adapted from Bannister and Calabrese,<sup>4</sup> SOD activity was quantified by inhibiting the oxidation of adrenaline and measured in a SpectraMax i3xELISA reader at 480 nm. Values were expressed as unit SOD/mg protein (U/mg protein). Glutathione levels were measured through a reaction between DTNB and thiols, promoting color development as a result. Total glutathione (GSH) levels were expressed in  $\mu$ mol per mg of protein-based on absorbance at 412 nm.<sup>21</sup>

### Protein Content

The protein content was determined using the Folin phenol reagent (phosphomolybdic-phosphotungstic reagent) by Lowry *et al.*<sup>31</sup> The bovine serum albumin was used to perform a standard curve. The results were expressed as mg protein (mg).

### Statistical Analysis

Data are expressed as the mean  $\pm$  standard error of the mean (SEM). Data were assessed for normal distribution using the Shapiro–Wilk test, and for homoscedasticity using Levene's test. Then, data were analyzed statistically by one-way analysis of variance (ANOVA) tests, followed by the Tukey *post hoc* test. The significance level for statistical tests is  $p < 0.05$ . SPSS (Statistical Package for the Social Sciences) version 17.0 was used.

## RESULTS

### Wound Contraction Analysis

Figure 1a shows representative images of the wound sizes. Figures 1b and 1c represent the wound contraction area in  $\text{cm}^2$ . On the 7th day after wound induction (Fig. 1b) the groups showed no significant difference. However, when analyzed on the 14th day after wound induction (Fig. 1c), it was possible to see a significant increase in wound contraction in the EW + AM and EW + AM + HA ( $p < 0.01$  and  $p < 0.001$ , respectively) groups compared to the Excisional Wound (EW) group.



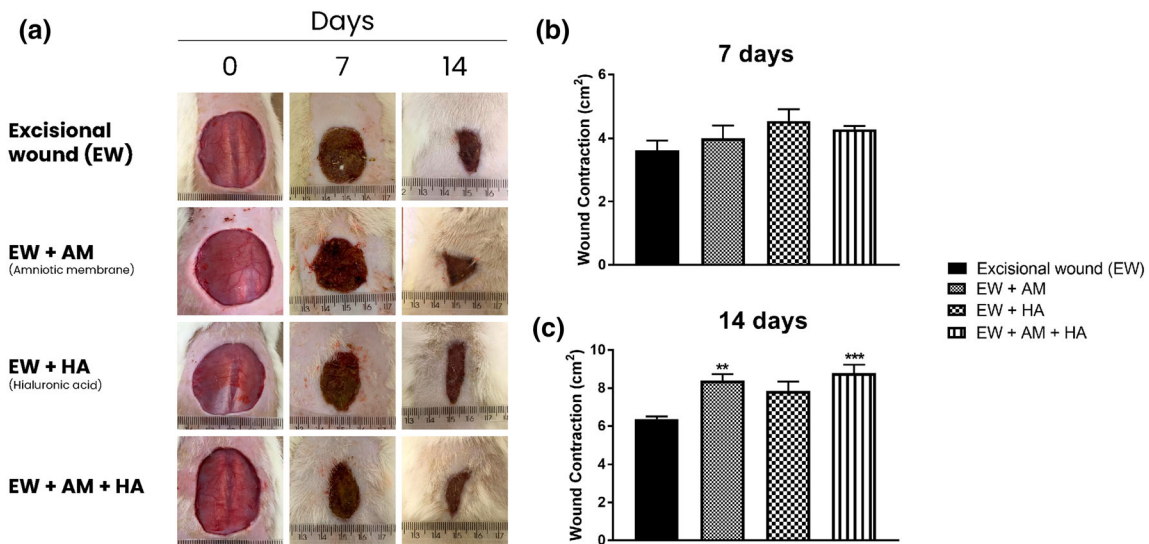


**FIGURE 1.** Effects of treatment with amniotic membrane and hyaluronic acid on wound contraction parameters where (a) representative images of the wound sizes; (b) wound contraction at 7 days; (c) wound contraction at 14 days. Data are presented as mean + SEM, in which: \* $p < 0.05$  vs. EW Group; \*\* $p < 0.01$  vs. EW Group; \*\*\* $p < 0.001$  vs. EW Group; columns which no symbol are non-significant; (One-way ANOVA followed by Tukey *post hoc* test).

### Histological Analysis

Figure 2a shows representative images of histological sections of the integumentary system on the 7th day after wound induction, which were quantified for the mean number of inflammatory infiltrate (Fig. 2b) and the mean number of blood vessels (Fig. 2c), which showed no significant difference. The mean number of fibroblasts (Fig. 2d) showed a significant increase in the combined therapy group (EW + AM + HA) compared to the EW group, while in the analysis of collagen fiber compaction (Fig. 2e) there was a significant increase in the EW + AM group when compared to control.

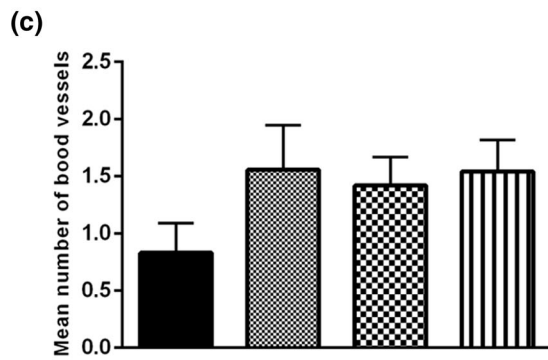
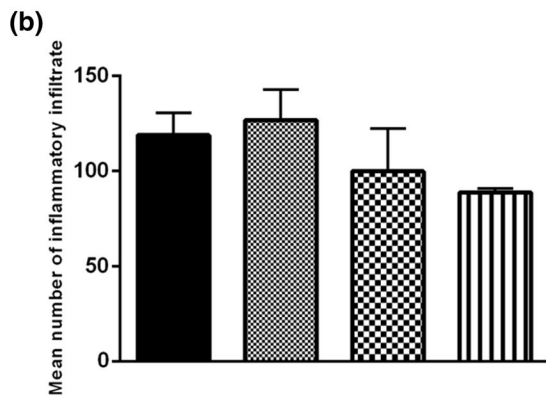
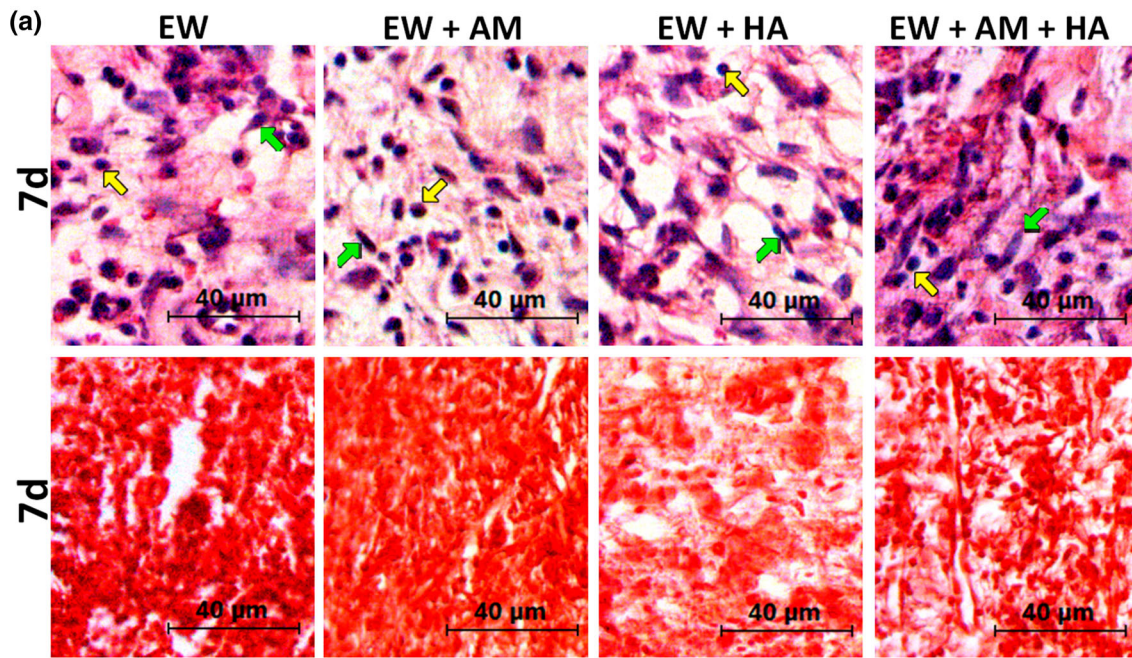
Figure 3a shows representative images of histological sections of the integumentary system now on the 14th day after wound induction. When quantifying the mean number of inflammatory infiltrates (Fig. 3b), there was a significant decrease in the combined therapy group (EW + AM + HA) compared to the EW group. Regarding the mean number of blood vessels (Fig. 3c), the mean number of fibroblasts (Fig. 3d), and collagen fiber compaction (Fig. 3e) there was no significant difference.

### RT-PCR

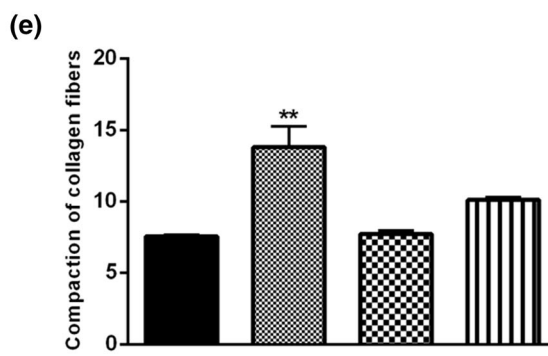
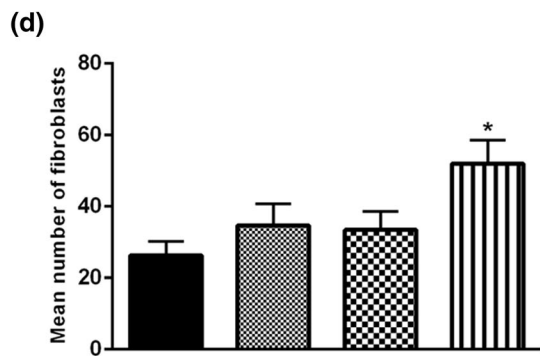
Figure 4 shows the analysis of gene expression of  $\text{Nf-}\kappa\beta$  and  $\text{Nrf2}$  markers on the 7th day after wound induction. When analyzing the content of  $\text{Nf-}\kappa\beta$  (Fig. 4a), there was a significant decrease in the EW + AM and EW + AM + HA groups when compared to the EW group ( $p < 0.05$ ). In the analysis of  $\text{Nrf2}$  content (Fig. 4b), there was no significant difference between groups.

### Pro-Inflammatory Cytokines

Figure 5 shows the protein levels of the pro-inflammatory cytokines  $\text{TNF-}\alpha$ ,  $\text{IL1}\beta$ , and  $\text{IL6}$  on the 7th day after wound induction. When  $\text{TNF-}\alpha$  levels were evaluated (Fig. 5a), there was a significant decrease in the EW + AM and EW + AM + HA groups compared to the EW group, and this difference was greater ( $p < 0.01$ ) for the EW + AM group. On the other hand,  $\text{IL1}\beta$  levels (Fig. 5b) showed a significant decrease only in the EW + AM + AH group when compared to the EW group. As for the cytokine



Excisional wound (EW)  
 EW + AM  
 EW + HA  
 EW + AM + HA



◀ **FIGURE 2.** Effects of treatment with amniotic membrane and hyaluronic acid on parameters of histological analysis on the 7th day. (a) Representative photomicrograph ( $\times 400$  magnification) of histological sections of wound area (Superior line: HE stained images, inflammatory infiltrate highlighted by yellow arrows and fibroblasts by green arrows. Inferior line: Ponceau S-stained images, highlighting the total collagen stained in red and its compaction). Mean number of (B) inflammatory infiltrate; (c) blood vessels; (d) fibroblasts; (e) total collagen compaction. Data are presented as mean + SEM, in which: \* $p < 0.05$  vs. EW Group; \*\* $p < 0.01$  vs. EW Group; columns which no symbol are non-significant; (One-way ANOVA followed by Tukey *post hoc* test).

IL6 (Fig. 5c), there was a significant decrease ( $p < 0.01$ ) in all groups when compared to the EW group.

Now as for the evaluation of pro-inflammatory cytokines on the 14th day after wound induction, TNF- $\alpha$  levels (Fig. 6) showed a significant decrease in all groups compared to the EW group ( $p < 0.001$ ), as well as the IL1 $\beta$  levels (Fig. 6b), in which there was a significant decrease in all groups compared to the EW group ( $p < 0.01$ ), and in the EW + AM and EW + AM + HA groups the difference was significantly greater ( $p < 0.0001$ ). Regarding IL6 levels, there was no significant difference.

#### *Anti-Inflammatory Cytokines*

Figure 7 shows the protein levels of anti-inflammatory cytokines (IL10, IL4, and TGF- $\beta$ ) on the 7th day after wound induction. There was only a significant difference in IL4 levels (Fig. 7b) where there is a significant increase in the combined therapy group (EW + AM + HA) compared to the control.

Protein levels of anti-inflammatory cytokines on the 14th day after wound induction are shown in Fig. 8. A very significant increase in cytokine IL10 (Fig. 8a) was observed in the EW + AM + HA group compared to the EW group ( $p < 0.0001$ ); the same occurred with IL4 levels ( $p < 0.001$ ) (Fig. 8b).

The growth factor TGF- $\beta$  (Fig. 8c) showed a significant increase in the EW + AM and EW + AM + HA groups compared to the EW group, whereas the differences were of  $p < 0.01$  and  $p < 0.0001$ , respectively.

#### *Oxidative Parameters*

The analysis of oxidants, oxidative damage, and antioxidants was carried out in 7 and 14 days; Fig. 9 shows the results for the 7th day after wound induction.

To evaluate the oxidants, the levels of DCF and Nitrite were analyzed. DCF results (Fig. 9a) on the 7th day were not significantly different; on the other hand, nitrite levels (Fig. 9b) show a significant decrease in the EW + AM + HA group compared to the EW group ( $p < 0.05$ ).

To assess the oxidative damage, Carbonyl levels and Sulfhydryl content were measured. We obtained a significant reduction in the levels of carbonyl groups (Fig. 9c) in the EW + HA ( $p < 0.05$ ) and EW + AM + HA ( $p < 0.01$ ) groups when compared to the EW group. The sulfhydryl content (Fig. 9d) was not significantly different.

Regarding antioxidant effects, SOD and GSH enzymes were measured. SOD levels (Fig. 9e) showed a significant increase ( $p < 0.05$ ) in the combined therapy group (EW + AM + HA) compared to the control group; the same occurred with GSH levels ( $p < 0.01$ ).

Figure 10 shows the results of oxidative parameters on the 14th day after wound induction. It was observed that the results of the oxidants DCF and Nitrite (Figs. 10a, 10b) did not present any significant difference, as happened with the oxidative damage markers Carbonyl and Sulfhydryl (Figs. 10c, 10d).

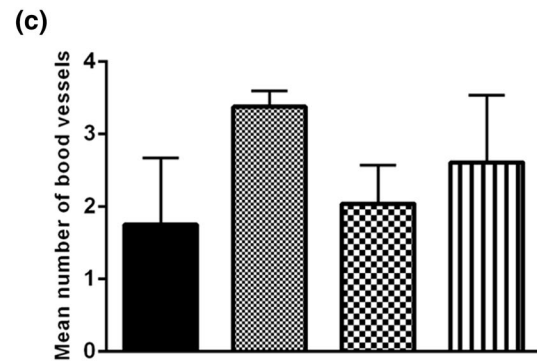
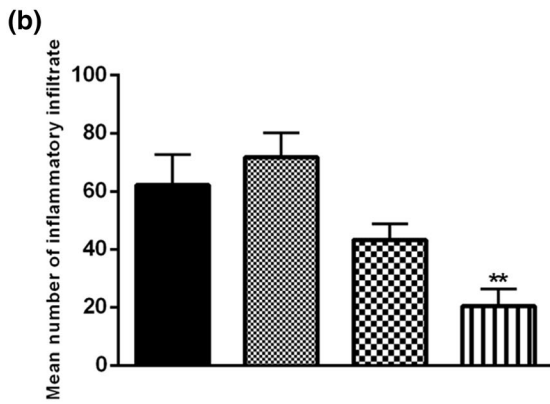
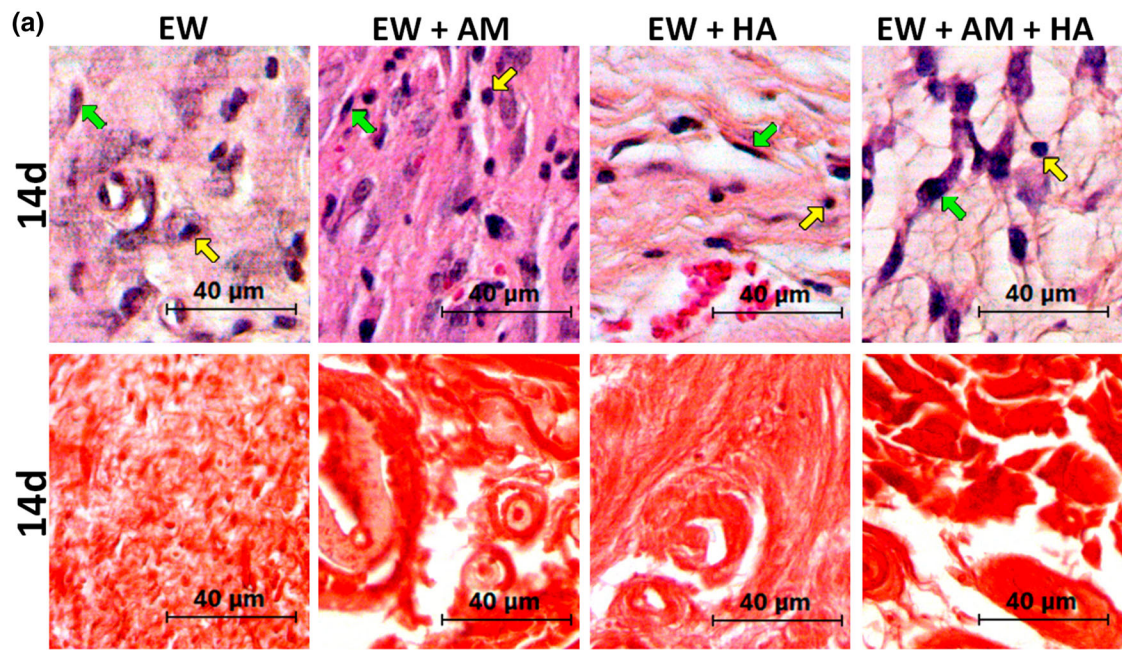
However, about the antioxidant system, the SOD and GSH enzymes were measured and both of them (Figs. 10e, 10f) showed a significant increase ( $p < 0.05$ ) in the combined therapy group (EW + AM + HA) in relation to the control.

## DISCUSSION

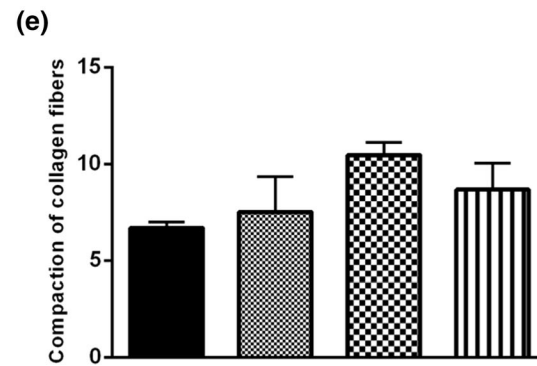
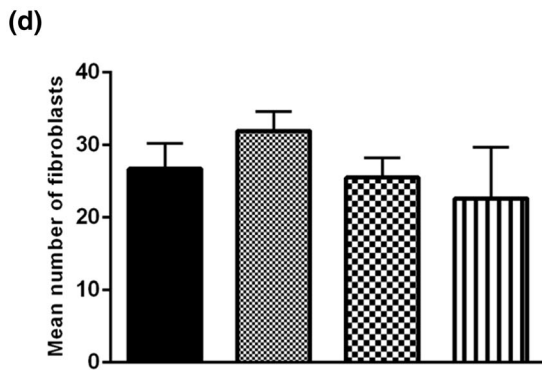
Deep wounds, which destroy the epidermis and part of the dermis, compromise oxygenation and the skin's ability to heal, accompanied by dehydration, shock, and infections. As these functional damages do not occur, immediate coverage is an essential measure in the treatment of wounds.

In this study, it was observed that the use of amniotic membrane solubilized with hyaluronic acid was able to accelerate wound healing, considering that there was a significant increase in the level of wound contraction in the groups that received this therapy both together and separately, as well as a significant increase in the number of fibroblasts and collagen fibers in the groups treated on the 7th day after wound induction. In addition, a reduction in the levels of the inflammatory marker NF- $\kappa\beta$ , of the pro-inflammatory cytokines TNF- $\alpha$ , IL1 $\beta$ , and IL6 were observed, while an increase in the anti-inflammatory cytokines IL10, IL4, and TGF- $\beta$  was observed in both on the 7th and





Excisional wound (EW)  
 EW + AM  
 EW + HA  
 EW + AM + HA





◀ **FIGURE 3.** Effects of treatment with amniotic membrane and hyaluronic acid on parameters of histological analysis on the 14th day. (a) Representative photomicrograph ( $\times 400$  magnification) of histological sections of wound area (Superior line: HE stained images, inflammatory infiltrate highlighted by yellow arrows and fibroblasts by green arrows. Inferior line: Ponceau S-stained images, highlighting the total collagen stained in red and its compaction). Mean number of (b) inflammatory infiltrate; (c) blood vessels; (d) fibroblasts; (e) total collagen compaction. Data are presented as mean + SEM, in which: \* $p < 0.05$  vs. EW Group; \*\* $p < 0.01$  vs. EW Group; columns which no symbol are non-significant; (One-way ANOVA followed by Tukey *post hoc* test).

14th days. There was also a decrease in reactive nitrogen species in the combined therapy group compared to the control on the 7th day of this study, along with a reduction in the levels of the oxidative damage marker carbonyl and an increase in the activity of the antioxidant enzymes SOD and GSH.

Data from Castellanos *et al.*<sup>8</sup> proposed that AM may affect wound healing by speeding up the migration of keratinocytes from the wound edge and that growth factors and progenitor cells released by AM may mediate the stimulatory effect on epithelialization, as well as Zhao *et al.*<sup>43</sup> reported that growth factors and cytokines are responsible for the effect of AM on cell migration. Chrissouli *et al.*<sup>10</sup> showed that amnion cells could stimulate fibroblast proliferation during wound healing. These effects can be attributed to the presence of growth factors in the amniotic fluid, especially FGF (fibroblast growth factor) and PDGF (platelet-derived growth factor).<sup>36</sup>

It is suggested that the healing process in this study occurred properly due to the joint effects of the amniotic membrane and hyaluronic acid. Hyaluronic acid mediates cell migration, adhesion, proliferation, and differentiation and is also an extracellular signaling molecule. In addition, it has shown extensive pharmacological activities, including immunoregulatory, anti-inflammatory, antioxidant, and anti-aging.

Studies have indicated that AM influences the NF- $\kappa$ B pathway through interactions with IKK $\alpha/\beta$  subunits, resulting in suppressed P-Ik $\beta$  phosphorylation and decreased NF- $\kappa$ B phosphorylation.<sup>5</sup> Further studies have suggested that high-molecular-weight HA also downregulates NF- $\kappa$ B *via* its CD44 receptor.<sup>2</sup>

The decrease in pro-inflammatory cytokines is important given that these mediators can cause apoptosis and decrease fibroblast proliferation, resulting in delayed wound healing.<sup>26</sup> The increase in anti-inflammatory cytokines is essential for the final repair of the wound, since collagen fibers, the main functional component of the dermal tissue layer and essential for wound resistance, are promoted by TGF- $\beta$ ; and IL-10 plays an important role in controlling inflammation, immune-mediated tissue damage, and reducing wound healing potential,<sup>35</sup> as well as suppressing the release and function of several pro-inflammatory cytokines such as IL1, TNF- $\alpha$ , and IL6, which is a normal endogenous feedback factor for the control of immune and inflammatory responses.<sup>33</sup>

Although AM contains a wide range of growth factors, cytokines, and extracellular matrix components, its therapeutic actions are principally attributed to a molecular complex known as HC-HA/PTX3,<sup>6,39</sup> a heavy chain complex that significantly promotes apoptosis of neutrophils and newly isolated macrophages after activated but sparing resting neutrophils, a process essential to resolve inflammation.<sup>39</sup> In addition, high molecular weight hyaluronic acid also promotes anti-inflammatory effects through other receptors such as CD44 and RHAMM. By binding to the CD44 receptor, it downregulates the expression of pro-inflammatory cytokines, and prostaglandins, and suppresses NF- $\kappa$ B activation.<sup>2</sup>

The inflammatory process leads to the release of ROS (reactive oxygen species), which contribute to the pathogenesis of wounds as they are highly reactive and cytotoxic. When ROS production is exacerbated, it causes oxidative stress, which has been linked to delayed wound healing, as it can cause the persistent release of pro-inflammatory cytokines, alter and/or destroy ECM proteins, and affect the functioning of fibroblasts and keratinocytes.<sup>14</sup> It has been suggested that AM is capable of removing ROS from its environment and exhibits evidence of its scavenger action, that is, its ability to neutralize free radicals.<sup>7,29</sup> Evidence also suggests that high molecular weight hyaluronic acid is a powerful anti-inflammatory molecule that can also neutralize intra and extracellular ROS.<sup>34</sup>

Analyzing the results as a whole, it is assumed that the proposed therapies acted together so that there was

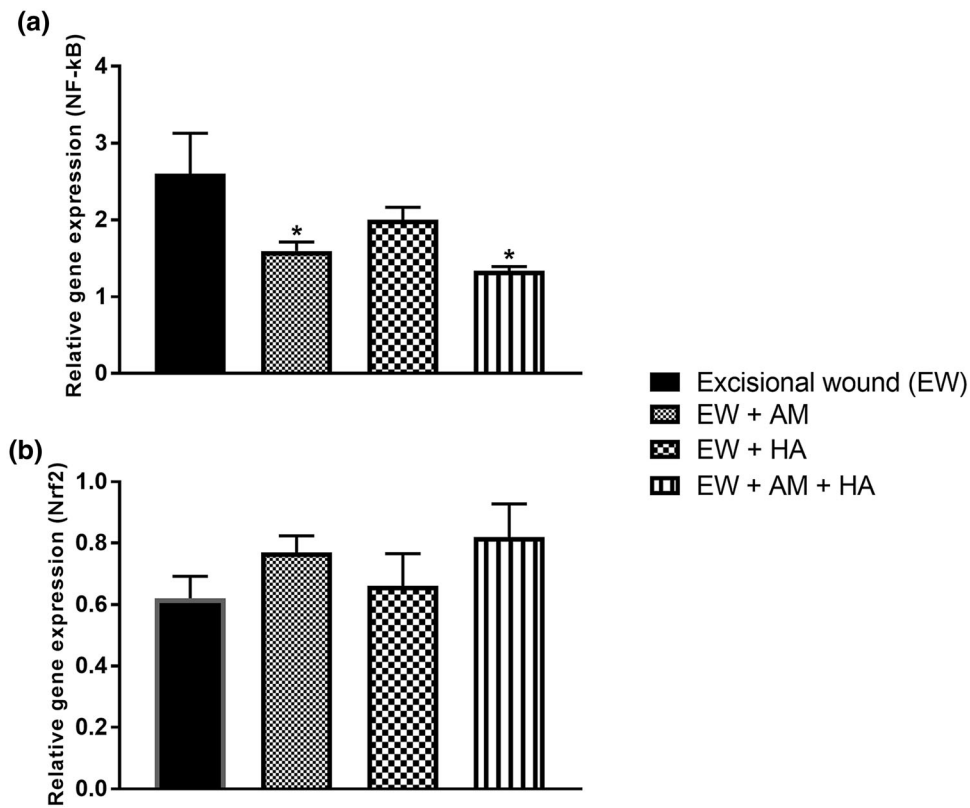


FIGURE 4. Effects of treatment with amniotic membrane and hyaluronic acid on parameters of gene expression of Nf-k $\beta$  and Nrf2 on the 7th day where (a) Nf-k $\beta$ ; (b) Nrf2. Data are presented as an average + SEM, in which: \* $p < 0.05$  vs. EW Group; columns which no symbol are non-significant; (One-way ANOVA followed by Tukey *post hoc* test).

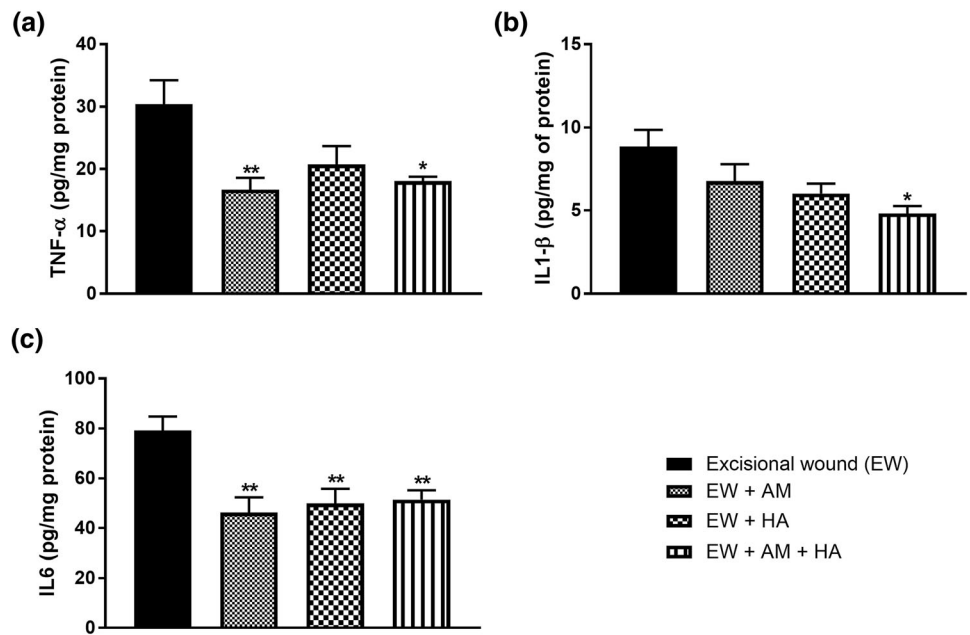


FIGURE 5. Effects of treatment with amniotic membrane and hyaluronic acid on parameters of pro-inflammatory cytokines on the 7th day in which (a) TNF- $\alpha$ ; (b) IL1 $\beta$ ; (c) IL6. Data are presented as mean + SEM, in which: \* $p < 0.05$  vs. EW Group; \*\* $p < 0.01$  vs. EW Group; columns which no symbol are non-significant; (One-way ANOVA followed by Tukey *post hoc* test).

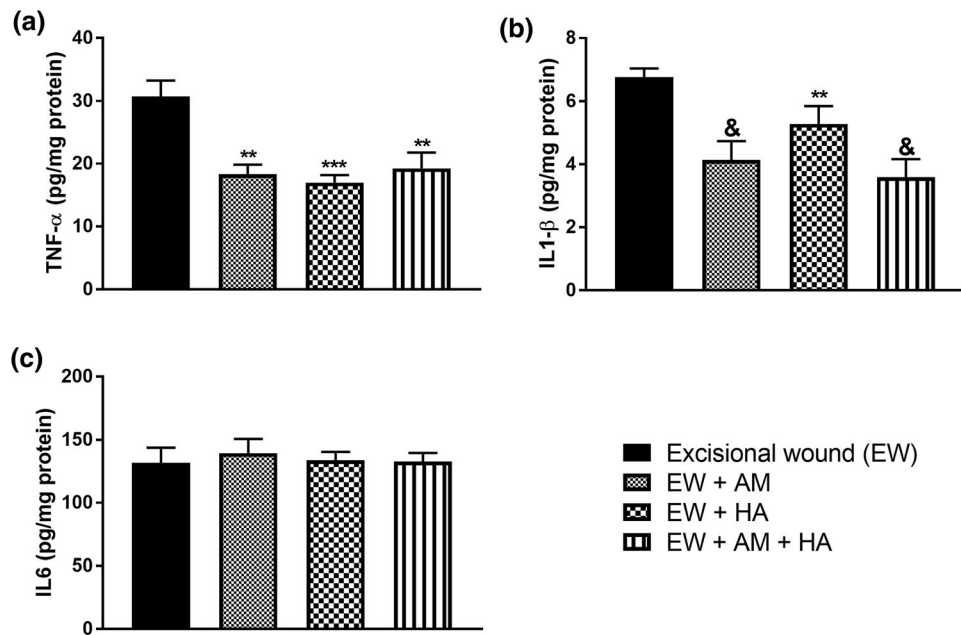


FIGURE 6. Effects of treatment with amniotic membrane and hyaluronic acid on pro-inflammatory cytokine parameters on the 14th day where (a) TNF- $\alpha$ ; (b) IL1 $\beta$ ; (c) IL6. Data are presented as mean + SEM, in which: \* $p$  < 0.05 vs. EW Group; \*\* $p$  < 0.01 vs. EW Group; \*\*\* $p$  < 0.001 vs. EW Group; & $p$  < 0.0001 vs. EW Group; columns which no symbol are non-significant; (One-way ANOVA followed by Tukey *post hoc* test).

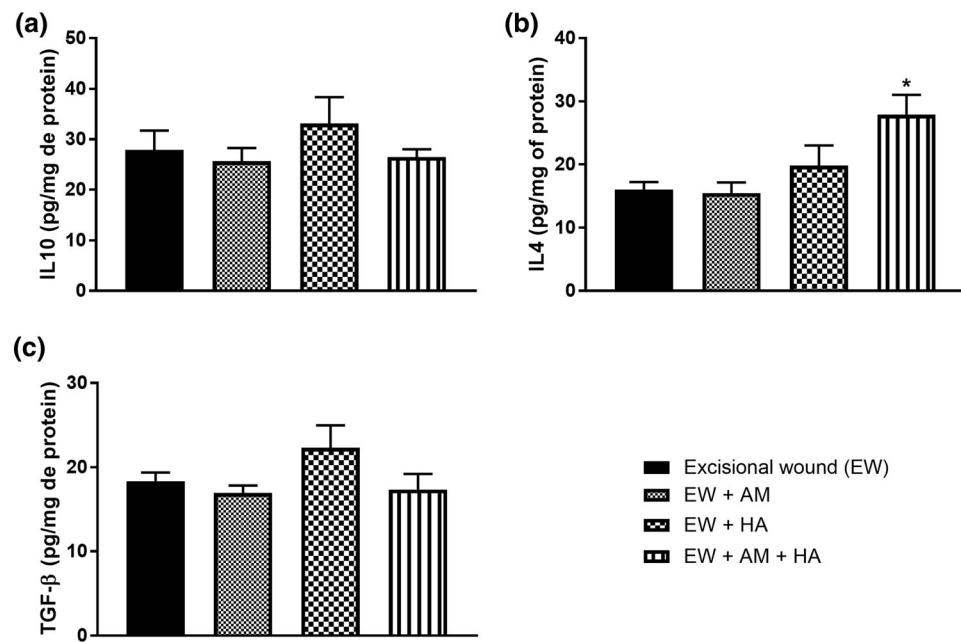
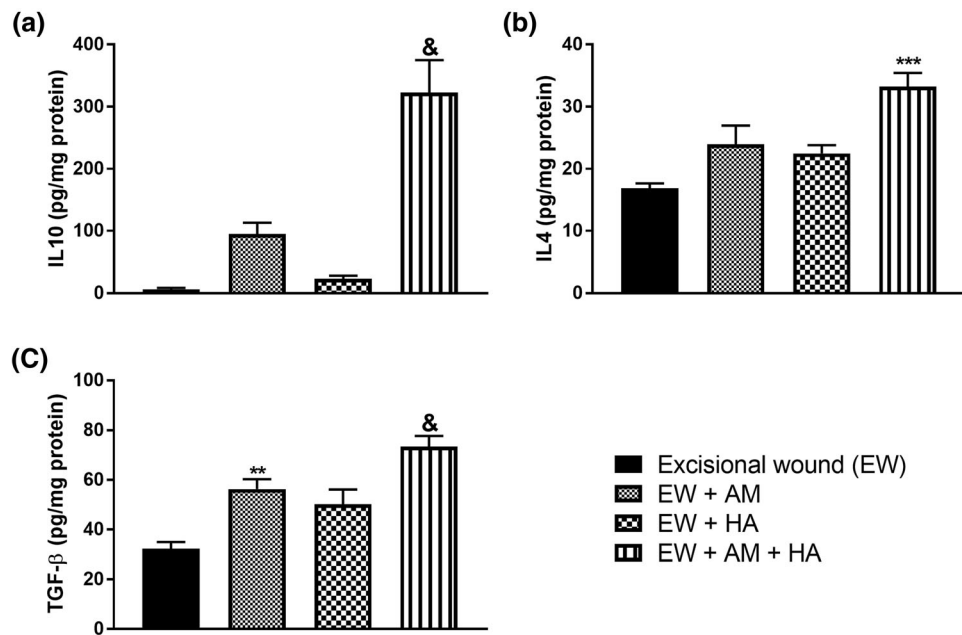


FIGURE 7. Effects of treatment with amniotic membrane and hyaluronic acid on anti-inflammatory cytokine parameters on the 7th day where (a) IL10; (b) IL4; (c) TGF- $\beta$ . Data are presented as mean + SEM, in which: \* $p$  < 0.05 vs. EW Group; columns which no symbol are non-significant; (One-way ANOVA followed by Tukey *post hoc* test).





**FIGURE 8.** Effects of amniotic membrane and hyaluronic acid treatment on anti-inflammatory cytokine parameters on the 14th day where (a) IL10; (b) IL4; (c) TGF- $\beta$ . Data are presented as mean + SEM, in which: \* $p < 0.05$  vs. EW Group; \*\* $p < 0.01$  vs. EW Group; \*\*\* $p < 0.001$  vs. EW Group; & $p < 0.0001$  vs. EW Group; columns which no symbol are non-significant; (One-way ANOVA followed by Tukey *post hoc* test).

an acceleration of the inflammatory process for the repair phase, with an increase in wound contraction, reduction of the NF- $\kappa$ B marker, reduction of pro-inflammatory cytokines, increase in anti-inflammatory cytokines and attenuation of oxidative stress, in addition to an increase in the number of fibroblasts and collagen fibers, indicating the effectiveness of the healing process.

## CONCLUSION

In conclusion, the present study demonstrated that the proposed combination of amniotic membrane and hyaluronic acid therapy favors the tissue repair process

of the epithelial lesion. The results showed a reduction in pro-inflammatory cytokines, an increase in anti-inflammatory cytokines, an increase in TGF- $\beta$ , and attenuation of oxidative stress, reducing the acute inflammatory response and promoting the beginning of tissue repair.

The use of the amniotic membrane for the treatment of wounds shows promise according to its various mechanisms of action and mainly due to its rich composition of auxiliary factors for the healing process, even more so when associated with hyaluronic acid, which has already been used in this area. Future studies using these treatments will be valid for a better understanding of their mechanisms, including collagen metabolism and M1 and M2 phenotyping, in addition to discovering other possible uses, as it provides many

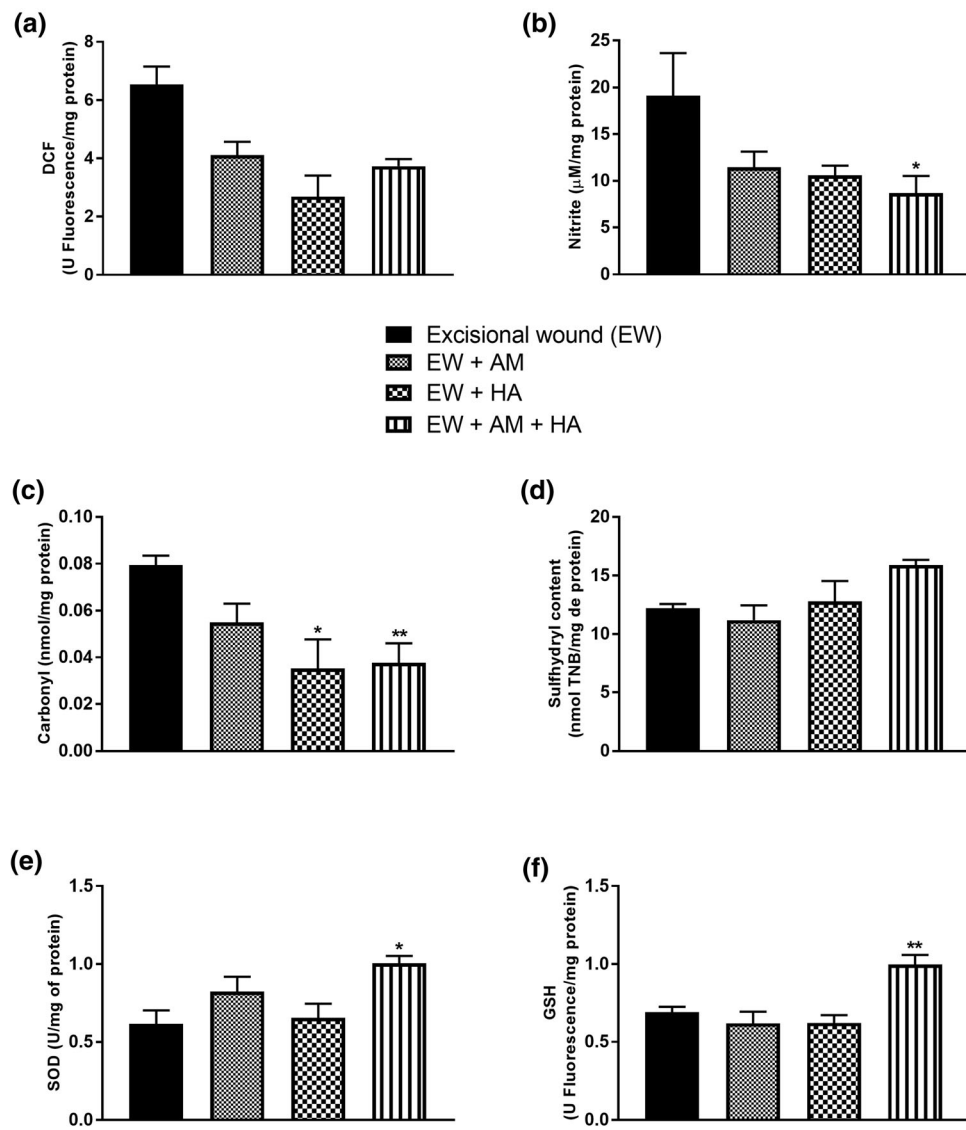


**FIGURE 9.** Effects of treatment with amniotic membrane and hyaluronic acid on oxidative parameters on the 7th day in which (a) DCF; (b) Nitrite; (c) Carbonyl; (d) Sulphydryl content; (e) SOD; (f) GSH. Data are presented as mean + SEM, in which: \* $p < 0.05$  vs. EW Group; \*\* $p < 0.01$  vs. EW Group; columns which no symbol are non-significant; (One-way ANOVA followed by Tukey *post hoc* test).

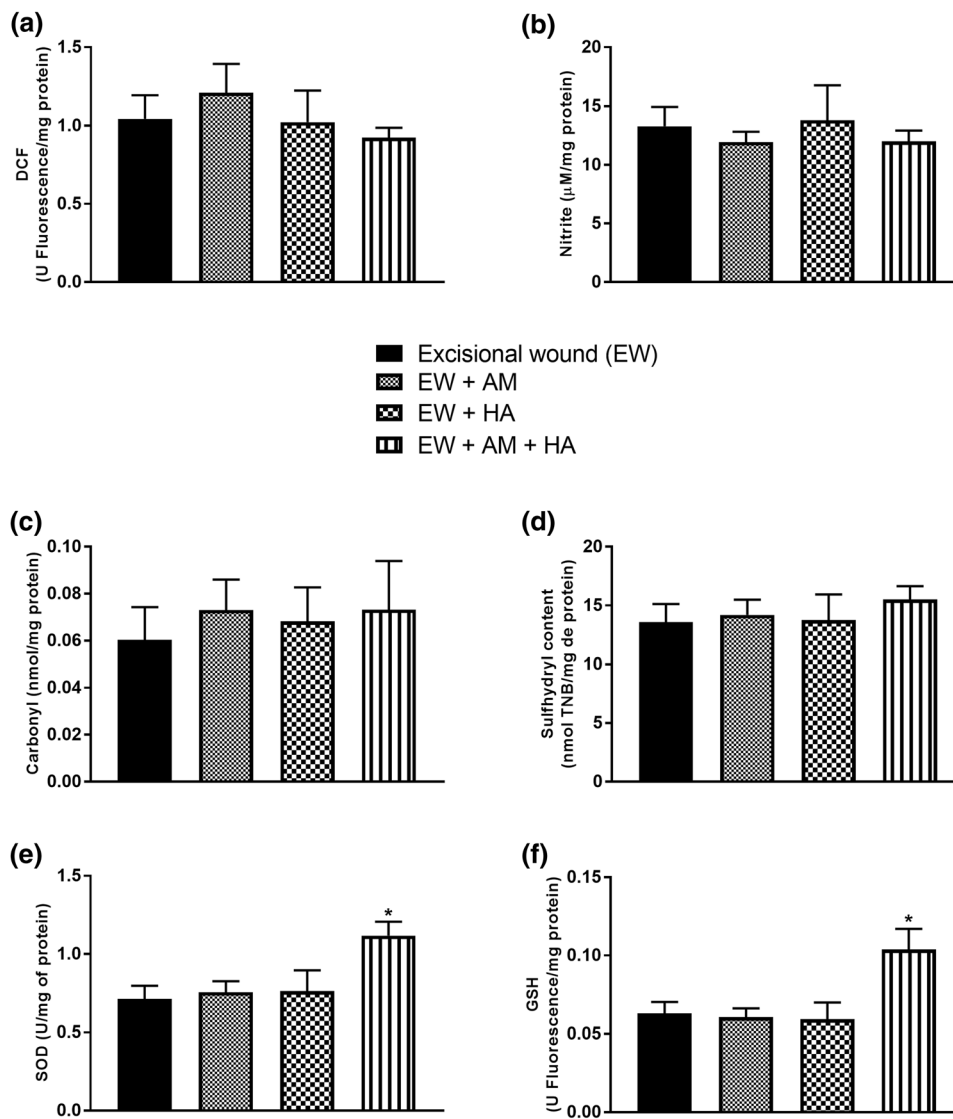


**FIGURE 10.** Effects of treatment with amniotic membrane and hyaluronic acid on oxidative parameters on the 14th day in which (a) DCF; (b) Nitrite; (c) Carbonyl; (d) Sulphydryl content; (e) SOD; (f) GSH. Data are presented as mean + SEM, in which: \* $p < 0.05$  vs. EW Group; \*\* $p < 0.01$  vs. EW Group; columns which no symbol are non-significant; (One-way ANOVA followed by Tukey *post hoc* test).

resources in its components that can be used in the treatment of various diseases.

#### ACKNOWLEDGMENTS

This work was supported by grants from Conselho Nacional de Desenvolvimento Científico e Tecnológico (CNPQ), Fundação de Amparo à Pesquisa e Inovação do Estado de Santa Catarina (FAPESC) and Universidade do Extremo-Sul Catarinense (UNESC).

#### DATA AVAILABILITY

The data that support the findings of this study are available upon reasonable request from the authors.

#### CONFLICT OF INTEREST

The authors have no conflict of interest to declare.



## REFERENCES

- <sup>1</sup>Aksenov, M. Y., and W. R. Markesbery. Changes in thiol content and expression of glutathione redox system genes in the hippocampus and cerebellum in Alzheimer's disease. *Neurosci. Lett.* 302:141–145, 2001.
- <sup>2</sup>Altman, R., A. Bedi, A. Manjoo, F. Niazi, P. Shaw, and P. Mease. Anti-inflammatory effects of intra-articular hyaluronic acid: a systematic review. *Cartilage.* 10:43–52, 2019.
- <sup>3</sup>Andrade, T. A. M., D. S. Masson-Meyers, G. F. Caetano, V. A. Terra, P. P. Ovidio, A. A. Jordão-Júnior, and M. A. C. Frade. Skin changes in streptozotocin-induced diabetic rats. *Biochem. Biophys. Res. Commun.* 490:1154–1161, 2017.
- <sup>4</sup>Bannister, J. V., and L. Calabrese. Assays for superoxide dismutase. *Methods Biochem. Anal.* 32:279–312, 1987.
- <sup>5</sup>Bauer, D., M. Hennig, S. Wasmuth, H. Baehler, M. Busch, K.-P. Steuhl, S. Thanos, and A. Heiligenhaus. Amniotic membrane induces peroxisome proliferator-activated receptor- $\gamma$  positive alternatively activated macrophages. *Investig. Ophthalmol. Vis. Sci.* 53:799–810, 2012.
- <sup>6</sup>Bennett, D. S. Cryopreserved amniotic membrane and umbilical cord particulate for managing pain caused by facet joint syndrome: a case series. *Medicine.* 98:e14745, 2019.
- <sup>7</sup>Burlingame, J. M., N. Esfandiari, R. K. Sharma, E. Mascha, and T. Falcone. Total antioxidant capacity and reactive oxygen species in amniotic fluid. *Obstet. Gynecol.* 101:756–761, 2003.
- <sup>8</sup>Castellanos, G. Amniotic membrane application for the healing of chronic wounds and ulcers. *Placenta.* 59:146–153, 2017.
- <sup>9</sup>Chae, I. H., K. W. Park, H. S. Kim, and B. H. Oh. Nitric oxide-induced apoptosis is mediated by Bax/Bcl-2 gene expression, transition of cytochrome c, and activation of caspase-3 in rat vascular smooth muscle cells. *Clin. Chim. Acta.* 341:83–91, 2004.
- <sup>10</sup>Chrissouli, S., H. Pratsinis, V. Velissariou, A. Anastasiou, and D. Kletsas. Human amniotic fluid stimulates the proliferation of human fetal and adult skin fibroblasts: the roles of bFGF and PDGF and of the ERK and Akt signaling pathways. *Wound Repair Regen.* 18:643–654, 2010.
- <sup>11</sup>Corrêa, M. E. A. B., D. P. dos Santos Hauptenthal, C. Mendes, R. P. Zaccaron, L. de RochCasagrande, L. M. Venturini, G. D. Porto, J. V. S. Bittencourt, J. I. de Souza Silva, and S. de Sousa Mariano. Effects of percutaneous collagen induction therapy associated with hyaluronic acid on inflammatory response, oxidative stress, and collagen production. *Inflammation.* 43:2232–2244, 2020.
- <sup>12</sup>Curtolo, G., J. de Paula Araújo, J. A. Lima, J. V. Brandt, J. V. S. Bittencourt, L. M. Venturini, P. C. L. Silveira, S. Rogers, C. M. Franzini, and V. F. F. de Goes. Silver nanoparticles formulations for healing traumatic injuries in oral mucosa of rats. *Arch. Oral Biol.* 129:105202, 2021.
- <sup>13</sup>Dong, J., K. K. Sulik, and S. Y. Chen. The role of NOX enzymes in ethanol-induced oxidative stress and apoptosis in mouse embryos. *Toxicol. Lett.* 193:94–100, 2010.
- <sup>14</sup>Dunnill, C., T. Patton, J. Brennan, J. Barrett, M. Dryden, J. Cooke, D. Leaper, and N. T. Georgopoulos. Reactive oxygen species (ROS) and wound healing: the functional role of ROS and emerging ROS-modulating technologies for augmentation of the healing process. *Int. Wound J.* 14:89–96, 2017.
- <sup>15</sup>Elkhenany, H., A. El-Derby, M. AbdElkoudous, R. A. Salah, A. Lotfy, and N. El-Badri. Applications of the amniotic membrane in tissue engineering and regeneration: the hundred-year challenge. *Stem Cell Res. Ther.* 13:8, 2022.
- <sup>16</sup>Garfias, Y., V. Zaga-Clavellina, F. Vadillo-Ortega, M. Osorio, and M. C. Jimenez-Martinez. Amniotic membrane is an immunosuppressor of peripheral blood mononuclear cells. *Immunol. Investig.* 40:183–196, 2011.
- <sup>17</sup>Gholipourmalekabadi, M., B. Farhadhosseinabadi, M. Faraji, and M. R. Nourani. How preparation and preservation procedures affect the properties of amniotic membrane? How safe are the procedures? *Burns.* 46:1254–1271, 2020.
- <sup>18</sup>Groeber, F., M. Holeiter, M. Hampel, S. Hinderer, and K. Schenke-Layland. Skin tissue engineering—in vivo and in vitro applications. *Adv. Drug Deliv. Rev.* 63:352–366, 2011.
- <sup>19</sup>Groom, M., R. J. Shannon, D. Chakravarthy, and C. A. Fleck. An evaluation of costs and effects of a nutrient-based skin care program as a component of prevention of skin tears in an extended convalescent center. *J. Wound Ostomy Cont. Nurs.* 37:46–51, 2010.
- <sup>20</sup>Hintze, V., M. Schnabelrauch, and S. Rother. Chemical modification of hyaluronan and their biomedical applications. *Front. Chem.* 10:830671, 2022.
- <sup>21</sup>Hissin, P. J., and R. Hilf. A fluorometric method for determination of oxidized and reduced glutathione in tissues. *Anal. Biochem.* 74:214–226, 1976.
- <sup>22</sup>Holzer-Geissler, J. C. J., S. Schwingenschuh, M. Zacharias, J. Einsiedler, S. Kainz, P. Reisenegger, C. Holecek, E. Hofmann, B. Wolff-Winiski, H. Fahrngruber, T. Birngruber, L. P. Kamolz, and P. Kotzbeck. The impact of prolonged inflammation on wound healing. *Biomedicines.* 10:856, 2022.
- <sup>23</sup>Hopper, R. A. Acellularization of human placenta with preservation of the basement membrane: a potential matrix for tissue engineering. *Ann. Plast. Surg.* 51:598–602, 2003.
- <sup>24</sup>Jiang, X., H. Ge, C. Zhou, X. Chai, and H. Deng. The role of transforming growth factor  $\beta$ 1 in fractional laser resurfacing with a carbon dioxide laser. *Lasers Med. Sci.* 29:681–687, 2014.
- <sup>25</sup>Jorge, L. F., J. C. Francisco, N. Bergonse, C. Baena, K. A. T. Carvalho, E. Abdelwahid, J. R. F. Neto, L. F. P. Moreira, and L. C. Guarita-Souza. Tracheal repair with acellular human amniotic membrane in a rabbit model. *J. Tissue Eng. Regen. Med.* 12:e1525–e1530, 2018.
- <sup>26</sup>Kandhare, A. D., P. Ghosh, and S. L. Bodhankar. Nar- ingin, a flavanone glycoside, promotes angiogenesis and inhibits endothelial apoptosis through modulation of inflammatory and growth factor expression in diabetic foot ulcer in rats. *Chem. Biol. Interact.* 219:101–112, 2014.
- <sup>27</sup>Levine, R. L., D. Garland, C. N. Oliver, A. Amici, I. Climent, A. G. Lenz, B. W. Ahn, S. Shaltiel, and E. R. Stadtman. Determination of carbonyl content in oxidatively modified proteins. *Methods Enzymol.* 186:464–478, 1990.
- <sup>28</sup>Lindholm, C., and R. Searle. Wound management for the 21st century: combining effectiveness and efficiency. *Int. Wound J.* 13:5–15, 2016.
- <sup>29</sup>Lockington, D., P. Agarwal, D. Young, M. Caslake, and K. Ramaesh. Antioxidant properties of amniotic membrane: novel observations from a pilot study. *Can. J. Ophthalmol.* 49:426–430, 2014.
- <sup>30</sup>Longinotti, C. The use of hyaluronic acid based dressings to treat burns: a review. *Burns Trauma.* 2:2321–3868.142398, 2014.

- <sup>31</sup>Lowry, O. H., N. J. Rosebrough, A. L. Farr, and R. J. Randall. Protein measurement with the Folin phenol reagent. *J. Biol. Chem.* 193:265–275, 1951.
- <sup>32</sup>Mendes, C., D. P. dos Santos Haupenthal, R. P. Zaccaron, G. de BemSilveira, M. E. A. B. Corrêa, L. de RochCasa-grande, S. de Sousa Mariano, J. I. de Souza Silva, T. A. M. de Andrade, and P. E. Feuser. Effects of the association between photobiomodulation and hyaluronic acid linked gold nanoparticles in wound healing. *ACS Biomater. Sci. Eng.* 6:5132–5144, 2020.
- <sup>33</sup>Menon, R., L. Ismail, D. Ismail, M. Merialdi, S. J. Lombardi, and S. J. Fortunato. Human fetal membrane expression of IL-19 and IL-20 and its differential effect on inflammatory cytokine production. *J. Matern. Fetal Neonatal Med.* 19:209–214, 2006.
- <sup>34</sup>Meszaros, M., A. Kis, L. Kunos, A. D. Tarnoki, D. L. Tarnoki, Z. Lazar, and A. Bikov. The role of hyaluronic acid and hyaluronidase-1 in obstructive sleep apnoea. *Sci. Rep.* 10:1–9, 2020.
- <sup>35</sup>Nguyen, V.-L., C.-T. Truong, B. C. Q. Nguyen, T.-N.V. Vo, T.-T. Dao, V.-D. Nguyen, D.-T.T. Trinh, H. K. Huynh, and C.-B. Bui. Anti-inflammatory and wound healing activities of calophyllolide isolated from *Calophyllum inophyllum* Linn. *PLoS ONE*.12:e0185674, 2017.
- <sup>36</sup>Nouri, M., M. Ebrahimi, T. Bagheri, M. J. Fatemi, A. Najafbeygi, S. Araghi, and M. Molaei. Healing effects of dried and acellular human amniotic membrane and mepitelas for coverage of skin graft donor areas; a randomized clinical trial. *Bull. Emerg. Trauma.* 6:195, 2018.
- <sup>37</sup>Posnett, J., and P. J. Franks. The costs of skin breakdown and ulceration in the UK. In: *Skin Breakdown: The Silent Epidemic*, Hull: Smith & Nephew Foundation, 2007, pp. 6–12.
- <sup>38</sup>Schulze, U., U. Hampel, S. Sel, T. W. Goecke, V. Thäle, F. Garreis, and F. Paulsen. Fresh and cryopreserved amniotic membrane secrete the trefoil factor family peptide 3 that is well known to promote wound healing. *Histochem. Cell Biol.* 138:243–250, 2012.
- <sup>39</sup>Tseng, S. C. HC-HA/PTX3 purified from amniotic membrane as novel regenerative matrix: insight into relationship between inflammation and regeneration. *Investig. Ophthalmol. Vis. Sci.* 57:41–68, 2016.
- <sup>40</sup>Vidal, B., and M. Mello. Supramolecular order following binding of the dichroic birefringent sulfonic dye Ponceau SS to collagen fibers. *Biopolymers.* 78:121–128, 2005.
- <sup>41</sup>Wilkinson, H. N., and M. J. Hardman. Wound healing: cellular mechanisms and pathological outcomes. *Open Biol.*10:200223, 2020.
- <sup>42</sup>Zhang, L., G. Xu, Y. Wei, M. Yuan, Y. Li, M. Yin, C. Chen, G. Huang, B. Shu, and J. Wu. *In situ* scarless skin healing of a severe human burn wound induced by a hCTLA4Ig gene-transferred porcine skin graft. *Int. J. Med. Sci.* 19:952–964, 2022.
- <sup>43</sup>Zhao, B., J.-Q. Liu, Z. Zheng, J. Zhang, S.-Y. Wang, S.-C. Han, Q. Zhou, H. Guan, C. Li, and L.-L. Su. Human amniotic epithelial stem cells promote wound healing by facilitating migration and proliferation of keratinocytes via ERK, JNK and AKT signaling pathways. *Cell Tissue Res.* 365:85–99, 2016.

**Publisher's Note** Springer Nature remains neutral with regard to jurisdictional claims in published maps and institutional affiliations.